Colloid Polym Sci (2014) 292:1289–1296
DOI 10.1007/s00396-014-3184-1

ORIGINAL CONTRIBUTION

Polymer coatings for sensitive analysis of colloidal silica nanoparticles in water

Samar Alsudir · Edward P. C. Lai

Received: 26 January 2014 / Revised: 11 February 2014 / Accepted: 15 February 2014 / Published online: 12 March 2014
© Springer-Verlag Berlin Heidelberg 2014

Abstract A new analytical approach has been developed for the sensitive detection of trace nanomaterials in water using silica as model inorganic nanoparticles. Our novel approach is based on coating of the nanoparticles with a polymer to make them larger in size for better ultraviolet (UV) light absorption. These polymer-coated nanoparticles can be separated from the monomer and polymer by capillary electrophoresis (CE) due to differences in their ionic charge, size, and surface functionality. Controlled polymerization of 2-hydroxypropyl methacrylate (HPMA) on silica nanoparticles increased their UV detection sensitivity by 5–7-fold. A second coating with polydopamine produced an extra 2-fold increase of the UV detection sensitivity. With both polyhydroxypropyl methacrylate and polydopamine coatings, a significant total enhancement of 10–14-fold in detection sensitivity was attained. Alternatively, addition of bisphenol A or polyvinyl alcohol to the HPMA polymerization mixture resulted in 9–10-fold increase of SiO_2 detection sensitivity due to additional absorption of the UV detector light.

Keywords Capillary electrophoresis · Detection sensitivity · Nanomaterials · Polyhydroxypropyl methacrylate · Polydopamine · Silica nanoparticles

Abbreviations

AIBN	2,2′-azobis-2-isobutyronitrile
BGE	Background electrolyte
BPA	Bisphenol A
CE	Capillary electrophoresis
DA	Dopamine
DDW	Deionized distilled water
DLS	Dynamic light scattering
EOF	Electroosmotic flow
HPMA	2-hydroxypropyl methacrylate
MO	Mesityl oxide
NM	Nanomaterial
NP	Nanoparticle
PDA	Polydopamine
PHPMA	Poly (2-hydroxypropyl methacrylate)
PVA	Polyvinyl alcohol
SDS	Sodium dodecyl sulfate
SiO_2	Silica
SiO_2@PHPMA	Polyhydroxypropyl methacrylate-coated silica
SiO_2@PHPMA@PDA	Polydopamine/polyhydroxypropyl methacrylate-coated silica
TEM	Transmission electron microscopy
UV	Ultraviolet
wt.%	Percent by weight

S. Alsudir · E. P. C. Lai (✉)
Department of Chemistry, Ottawa-Carleton Chemistry Institute, Carleton University, Ottawa, ON K1S 5B6, Canada
e-mail: edward.lai@carleton.ca

Introduction

The industrial use of nanomaterials (NMs) and nanoparticles (NPs) in consumer products has proliferated, as found in electronic components [1], sports equipment [2], textile products [3], cosmetics [4], and biomedical applications [5–8]. Upon disposal of these products, these NMs often afford higher environmental mobility and will inevitably lead to a wide range of human exposure to aluminum oxide, carbon, copper oxide, gold, hematite, magnetite, manganese oxide [9], silver [10], titanium oxide [11], and polymer composite nanomaterials. The toxicity of NMs arises from a number of biophysicochemical factors, including their ability to penetrate biological barriers, tissues, and cells. Their large surface area-to-mass ratio increases oxidative stress, resulting in

undesirable interactions with biological macromolecules. Alumina and silica are among those inorganic NPs most often used in the industry even though their toxicity is controversial [12, 13]. Colloidal silica nanoparticles are more and more often used in various biomedical applications [14–16], and they are found in fresh water resources over a large range of concentrations [17]. Therefore, analytical techniques with high sensitivity are much sought after for the detection and quantification of these NPs. Measurement of the magnitude, frequency, and duration of exposure to these NMs is a critical first step in risk assessment. Unfortunately, it is difficult to build risk assessment scenarios for NMs due to the limited availability of sensitive methods for their detection and quantification.

Analytical methods for the analysis of NMs were recently addressed by Barceló and Farré [18, 19]. They gave a detailed overview of analytical methods and instruments suited for the separation, characterization, and quantification of various NMs and NPs in different matrices. Challenges arise generally from the diversity in their chemical properties and reactivities [20, 21]. Efforts have been focused in our lab to develop polymer growth on NPs as a novel method for their trace analysis in water. The coating material was chosen on the basis of several experimental considerations including simplicity of polymerization in aqueous solution, ability to interact with specific NPs, uniform dispersion of the coated NPs in water, strong ultraviolet (UV) absorptivity, and good electrophoretic mobility for separation by capillary electrophoresis (CE) with UV detection. CE offers various advantages including simplicity in operation, minute sample volumes, minimal consumption of environmentally unfriendly organic solvents, various separation modes, short analysis time, and the high resolution of complex mixtures, which results from having a uniform electroosmotic flow (EOF) [22]. Variance from run to run should not have an effect on the electrophoretic mobility of NMs and NPs as it is measured in relation to a neutral marker, unless there are time-dependent or non-equilibrium interactions of NMs with the capillary wall [23]. Characterization of NPs by CE had been successfully developed in our research lab [24]. Their UV detection limits remained inadequate for general application in environmental science and engineering studies.

In this work, aqueous polymerization of 2-hydroxypropyl methacrylate (HPMA) was investigated on silica (SiO_2) for better detection sensitivity in CE-UV analysis. An adhesive coating of polydopamine (PDA) was next put on top of the PHPMA-coated silica nanoparticles (SiO_2@PHPMA) to further enhance the detection sensitivity. Attempts were also made to decrease the rate of HPMA polymerization by adding polyvinyl alcohol (PVA) [25], thus increasing the PHPMA coating thickness on SiO_2 NPs. Finally, bisphenol A (BPA) was added to increase the UV absorbance of SiO_2@PHPMA for extra detection sensitivity.

Material and methods

Materials

2,2′-azobis-2-isobutyronitrile (AIBN) was bought from Pfaltz & Bauer (Waterbury, CT, USA). Bisphenol A (BPA), dopamine hydrochloride (DA.HCl, ≥99.5 %), 2-hydroxypropyl methacrylate (HPMA, 97 %), mesityl oxide (MO, ≥90 %), sodium dodecyl sulfate (SDS, ≥99 %), and LUDOX® colloidal silica (SiO_2, 30 % wt. suspension in H_2O, with a surface area of 198–250 m^2/g), and polyvinyl alcohol (PVA, with an average molecular weight of 10,000 and the degree of hydrolysis about 80 %.) were all purchased from Sigma-Aldrich (Oakville, ON, Canada). Sodium phosphate dibasic was obtained from Fisher Scientific (Fair Lawn, NJ, USA).

Apparatus and analytical method

CE-UV analyses were performed on a modular system built in our laboratory, which includes a Spellman CZE1000R high-voltage power supply (Hauppauge, NY, USA). Fused silica capillary (51 mm i.d., 356 mm o.d.) was obtained from Polymicro Technologies (Phoenix, AZ, USA). The capillary total and effective lengths were 53.5 and 46.1 cm, respectively. The background electrolyte (BGE) was composed of 10 mM Na_2HPO_4 in deionized distilled water (DDW) to attain pH 7.5 ±0.2. All CE analyses were run at an applied voltage of 20 kV, with the capillary inlet 2-mm away and below the electrode tip to improve both precision and baseline stability. A Bischoff Lambda 1010 (Leonberg, Germany) UV detector was set up at a wavelength of 190 nm to monitor the SiO_2 nanoparticles, polymer(s), and monomer(s). Electrokinetic injection at 17 kV for 12 s was employed to load the sample into the capillary for CE analysis. An independent run of MO as a neutral marker was carried out to determine the ionic charges of SiO_2 nanoparticles, polymer, and monomer. A PeakSimple chromatography data system (SRI model 203, Torrance, CA, USA) was used to acquire the detector output signal.

Polymerization of HPMA

Poly (2-hydroxypropyl methacrylate) (PHPMA) was prepared following a procedure developed by Ali et al. [26] with some modification. In a glass vial for free radical polymerization, HPMA (0.007 mol) was first dissolved in DDW (25 mL). SDS (10 wt.% of HPMA) and AIBN (3 wt.% of HPMA) were then added, followed by pure nitrogen gas bubbling for 5 min to remove dissolved oxygen molecules that could destroy the free radicals generated by thermal decomposition of AIBN. Finally, the vial was sealed and placed in a 60 °C thermostatted water bath for 22 h without further mixing or shaking. The polymerization mixture turned cloudy, yielding PHPMA submicron particles with a white color.

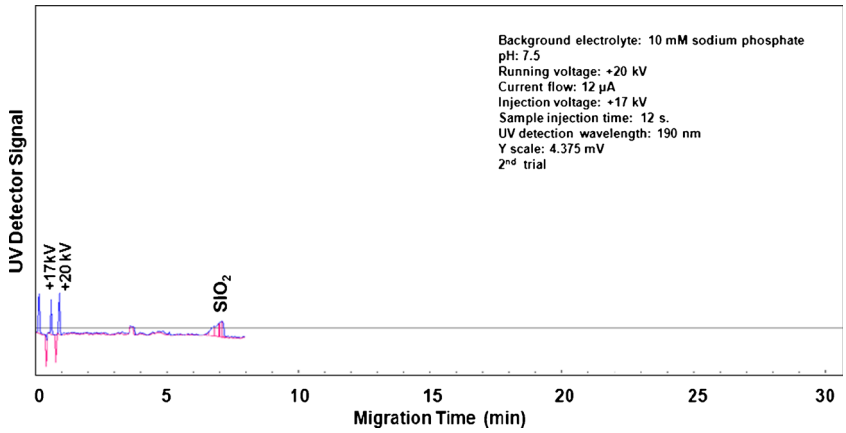

Fig. 1 CE-UV characterization of SiO_2 nanoparticles (at 20 g/L) in LUDOX® AM colloid

PHPMA growth on colloidal SiO_2 nanoparticles

HPMA (0.007 mol) was first dissolved in DDW (25 mL) containing colloidal SiO_2 nanoparticles (5–20 g/L). Sonication for 5 min was allowed to facilitate their hydrogen bonding interaction. Next, SDS (10 wt.% of HPMA) and AIBN (3 wt.% of HPMA) were added, followed by deoxygenation. Finally, the vial was placed in a 60 °C thermostatted water bath for 22 h to produce PHPMA-coated silica nanoparticles (SiO_2@ PHPMA) also with a white color.

Effect of AIBN on PHPMA growth

The amount of AIBN on PHPMA growth on SiO_2 nanoparticles was investigated by using 1, 2, and 3 wt.%. The percent conversion to PHPMA was determined by CE analysis for any residual HPMA.

Polydopamine growth on SiO_2@ PHPMA

Aqueous solution of DA (200 μL of 25 g/L) was added into SiO_2@PHPMA aqueous suspension. The mixture was left alone at ambient temperature (23±2 °C) to allow for PDA growth on the particles, as monitored by CE-UV analysis daily for 1 week.

Polymerization of HPMA with polyvinyl alcohol or bisphenol A

PVA (0.1 g) or BPA (0.2 g/L) was added to the HPMA polymerization mixture to investigate any enhancement of SiO_2 detection sensitivity.

Dynamic light scattering

The average diameters of original and polymer-coated SiO_2 particles were measured by dynamic light scattering (DLS) using a Brookhaven Instruments NanoDLS particle size analyzer (Holtsville, NY, USA), in ten replicates of 10 s each for higher accuracy.

Transmission electron microscopy

Dry SiO_2, SiO_2@PHPMA, and SiO_2@PHPMA@PDA particles were deposited on a sample holder for transmission electron microscopy (TEM) examination at an accelerating

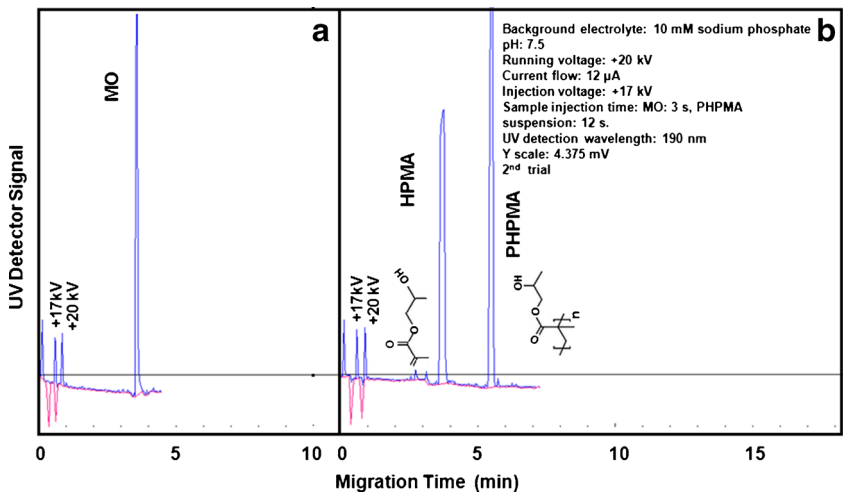

Fig. 2 CE-UV characterization of **a** MO and **b** HPMA (and PHPMA) after 22 h of polymerization

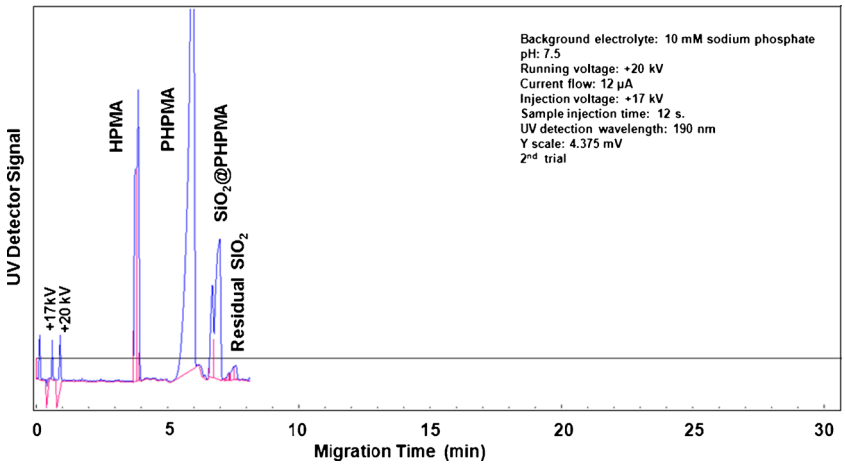

Fig. 3 CE-UV analysis of PHPMA and SiO_2@PHPMA particles after 22 h of polymerization using AIBN at 3 wt.%

voltage of 120–200 kV using an FEI Tecnai G2 transmission electron microscope (Hillsboro, OR, USA). The diameters of these particles were compared to determine the thickness of different coatings.

Results and discussion

Silica nanoparticles

LUDOX® AM colloidal silica nanoparticles [27] were prepared in the BGE for CE-UV analysis using electrokinetic injection. As shown in Fig. 1, 20 g/L of SiO_2 nanoparticles exhibited low UV absorbance at the UV detection wavelength of 190 nm, producing a small peak at the migration time of 7.0 ±0.1 min.

The SiO_2 nanoparticles appeared after the neutral marker, hence indicating their negative ionic charges (probably as SiO_4^{2-}) in the BGE and yielding a negative electrophoretic mobility value. The standard calibration curve exhibited a linear correlation coefficient (R^2=0.979) between their CE-UV peak area and concentration in the working range up to 20 g/L. The limit of detection (LOD at 3σ) and the limit of quantification (LOQ at 10σ) were determined to be 3 and 9 g/L, respectively, which are inadequate for many environmental science and engineering studies.

CE-UV characterization of PHPMA particles

CE-UV analysis was next performed on the HPMA polymerization mixture after 22 h at 60 °C. As a neutral compound illustrated in Fig. 2a, the residual HPMA migrated at nearly the electroosmotic flow velocity to appear at a time close to the 3.7 ±0.1 min for the neutral marker as shown in Fig. 2b. The late migration time of 5.6±0.1 min for PHPMA indicated its negative ionic charge in the BGE, possibly due to the adsorption of SDS anions on the hydrophobic polymer surface.

PHPMA growth on SiO_2 particles

Polymerization of HPMA at 60 °C was conducted for 22 h in the presence of SiO_2 nanoparticles over a range of concentrations from 5–20 g/L. The resultant SiO_2@PHPMA particles were analyzed by CE-UV to determine their electrophoretic mobility and detection sensitivity.

As shown in Fig. 3, a new peak for SiO_2@PHPMA particles was detected at a migration time of 6.8±0.1 min. These particles exhibited larger peak height and peak area than the original SiO_2 nanoparticles (see Fig. 1). Apparently, the SiO_2 nanoparticles were coated by PHPMA to have their $Si\text{-}O^-$ groups buried under the surface, thus resulting in faster migration than SiO_2 nanoparticles (at 7.5±0.1 min) and good separation from PHPMA (at 5.6±0.1 min). Upon varying the concentration of SiO_2 nanoparticles in the pre-polymerization mixture, the resultant SiO_2@PHPMA peak area changed accordingly as shown in Fig. 4, which provides very convincing proof of the SiO_2@PHPMA formation.

The LOD and LOQ for SiO_2@PHPMA particles were determined to be 0.6 and 1.8 g/L, respectively. Consequently,

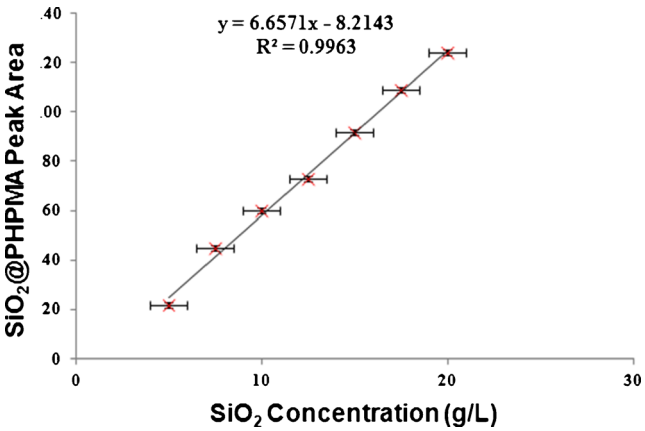

Fig. 4 SiO_2@PHPMA peak area obtained from different SiO_2 concentrations (g/L)

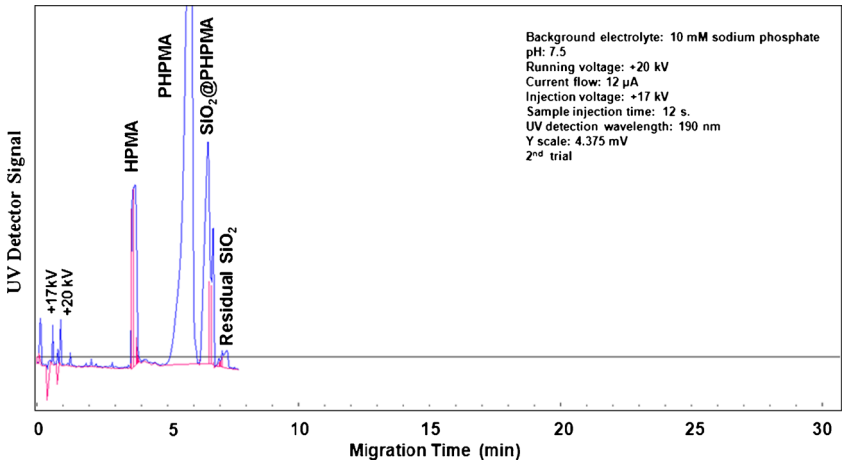

Fig. 5 CE-UV analysis of PHPMA and SiO_2@PHPMA particles after 22 h of polymerization using AIBN at 1 wt.%

a 5-fold better CE-UV detection sensitivity was attained for SiO_2 nanoparticles after PHPMA coating. Hence, the approach seemed promising toward their sensitive detection in water.

Effect of AIBN on PHPMA growth

Polymerization of HPMA to form a layer of PHPMA on SiO_2 nanoparticles was slightly increased from 94 to 96 % when the mount of AIBN (the initiator) was reduced from 3 to 1 wt.%. At 3 wt.%, a larger concentration of reactive radicals would be generated, leading to early termination of the polymerization process and production of a polymer of low molecular weight [28, 29]. On the contrary, at 1 wt.%, a chain carrier will be formed from the reaction of a free radical with a monomer unit and propagation will occur continuously with other monomer units present, resulting in a higher conversion of HPMA to PHPMA. Thereby, larger SiO_2@PHPMA particles were produced. A 33-% increase in SiO_2@PHPMA peak area was attained and the amount of residual SiO_2 nanoparticles was slightly reduced as shown in Fig. 5. Thus, PHPMA growth using AIBN at 1 wt.% resulted in 6–7-fold enhancement of SiO_2 detection sensitivity.

PDA growth on SiO_2@PHPMA particles in water

PDA growth on SiO_2@PHPMA particles in aqueous suspension over 1 week was investigated for further enhancement of detection sensitivity. The resultant SiO_2@PHPMA@PDA particles were analyzed by CE-UV daily. Figure 6 shows the CE-UV electropherogram of DA, HPMA, PHPMA@PDA, SiO_2@PHPMA@PDA, and residual SiO_2 particles. DA (at 3.2±0.1 min) is positively charged in the BGE as it migrated before the neutral marker. Hence, electrostatic attraction between DA and PHPMA or SiO_2@PHPMA particles were expected. Due to the adsorption of SDS anions on the hydrophobic polymer surface, PDA acquired a slight negative charge and migrated behind the neutral marker (as observed in a separate CE-UV analysis). After 7 days of polymerization, the suspension turned black as a result of PDA formation. Both the PHPMA@PDA peak at 7.0±0.1 min and SiO_2@PHPMA@PDA peak at 8.1±0.1 min increased in

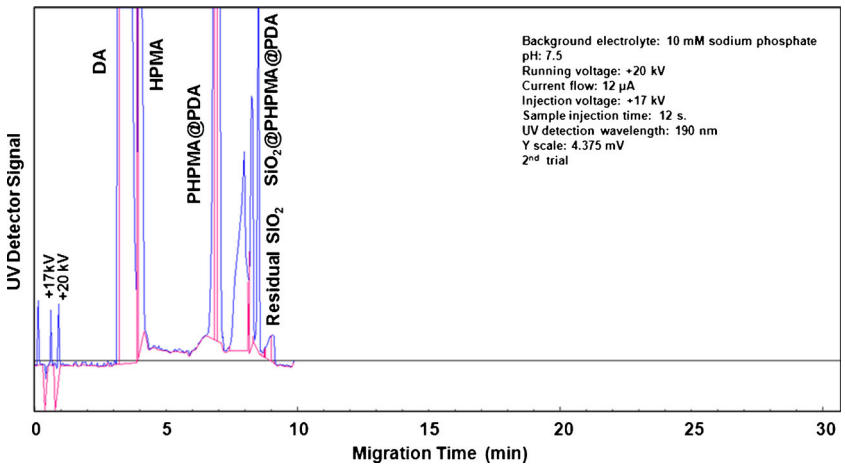

Fig. 6 CE-UV analysis of DA, HPMA, PHPMA@PDA, and SiO_2@PHPMA@PDA particles

Table 1 CE-UV peak areas of HPMA, PHPMA, and SiO_2@PHPMA under different conditions of HPMA polymerization. All peak areas are expressed in arbitrary units of mV.s

Condition of HPMA polymerization	Peak area of residual HPMA	Peak area of PHPMA	Peak area of SiO_2@PHPMA	% Polymerization of HPMA to form PHPMA
Without SiO_2 (AIBN at 3 wt.%)	32±1	57±1	–	~94
With SiO_2 (AIBN at 3 wt.%)	31±3	156±1	27±1	~94
Without SiO_2 (AIBN at 1 wt.%)	29±1	86±1	–	~95
With SiO_2 (AIBN at 1 wt.%)	25±1	221±10	40±3	~96
Without SiO_2+PVA	55±1	153±1	–	~90
With SiO_2+PVA	48±1	261±4	42±2	~91
Without SiO_2+BPA	98±1	102±2	–	~82
With SiO_2+BPA	185±1	258±6	47±1	~66

height and area upon PDA growth. Apparently, PHPMA and SiO_2@PHPMA particles were coated with a thin layer of PDA to be acquiring extra negative charges on their surfaces, rendering them slower in migration. This thin layer of PDA coating produced an extra 2-fold enhancement of the CE-UV detection sensitivity for SiO_2@PHPMA nanoparticles. Thus, with both PHPMA and PDA coatings, a total of 10–14-fold enhancement in detection sensitivity was attained for SiO_2 nanoparticles in the original sample.

Polymerization of HPMA with PVA or BPA

As shown in Table 1, the PHPMA peak areas attained in the presence of SiO_2 NPs under different conditions of polymerization were significantly larger than those obtained in the absence of SiO_2. The difference in PHPMA peak areas between the presence and absence of SiO_2 NPs was also significantly larger than the peak area of SiO_2@PHPMA. One speculation for this significant difference is the catalytic effect of SiO_2 NPs that could facilitate the HPMA polymerization and thus produce more PHPMA particles. Another speculation is the formation of a thick coating of PHPMA to cover up all the negative charges present on the SiO_2 surface, thus producing SiO_2@PHPMA particles with effectively the same migration time as PHPMA particles. Nonetheless, the SiO_2@PHPMA peak area and height were significantly larger than those of the original SiO_2 NPs. These SiO_2@PHPMA particles might have only a monolayer of PHPMA that could not cover up all the negative charges on SiO_2, and thus, they migrated after the PHPMA particles. Chu et al. had previously used PVA to decrease the rate of HPMA polymerization, thereby producing larger particles [25]. In our study, PVA increased the PHPMA peak area, which indicates the formation of larger PHPMA particles as confirmed by DLS analysis below. Addition of BPA also resulted in the formation of larger PHPMA particles. Consequently, PVA or BPA addition

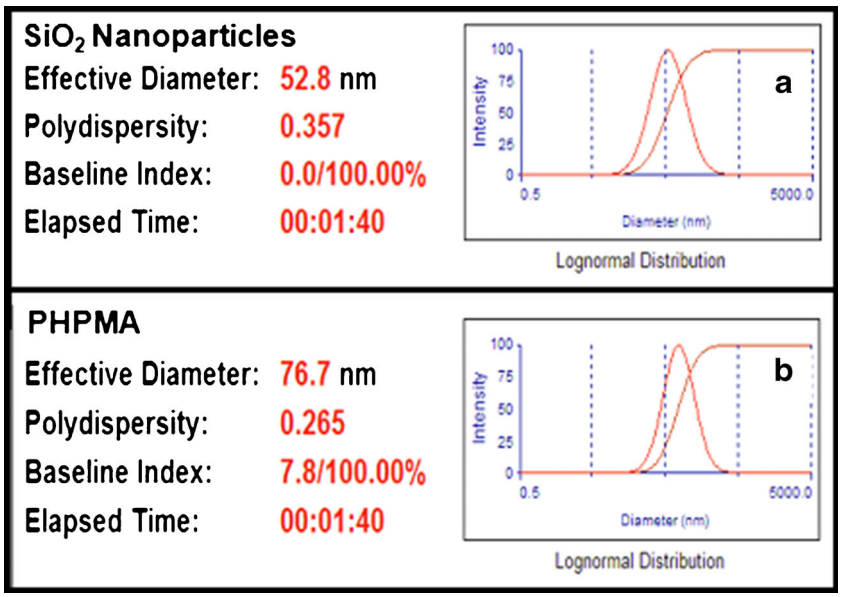

Fig. 7 Dynamic light scattering measurements of **a** lognormal distribution of SiO_2 nanoparticles in LUDOX® AM colloid and **b** lognormal distribution of PHPMA in DDW after 22 h of polymerization at 60 °C

Table 2 DLS measurement of the hydrodynamic diameters of original and polymer-coated SiO_2 particles

Particles	Hydrodynamic diameter (nm)
SiO_2	53±3
PHPMA (AIBN at 3 wt.%)	64±3
PHPMA (AIBN at 1 wt.%)	77±5
BPA-PHPMA	78±3
SiO_2@PHPMA (AIBN at 3 wt.%)	89±2
PVA-PHPMA	91±3
SiO_2@PHPMA (AIBN at 1 wt.%)	101±1
SiO_2@BPA-PHPMA	114±2
SiO_2@PVA-PHPMA	129±4
SiO_2@PHPMA@PDA	140±4

to the HPMA polymerization mixture containing SiO_2 NPs resulted in 9–10-fold increase of SiO_2 detection sensitivity probably due to additional absorption of the UV detector light.

Dynamic light scattering

Aqueous suspensions of original and polymer-coated SiO_2 particles were analyzed by DLS to determine their hydrodynamic diameters to gain some insight of their growth. The hydrodynamic diameter represents the actual particle diameter plus the hydration layer surrounding the particle as it moves under the influence of Brownian motion. As shown in Fig. 7a, b, mean diameters of 53±3 and 77±5 nm were obtained for SiO_2 nanoparticles and PHPMA particles, respectively. Larger particle diameters were exhibited by SiO_2@PHPMA, SiO_2@PHPMA@PDA, and SiO_2@PHPMA formed in the presence of BPA and PVA as summarized in Table 2. These results provide strong evidence that SiO_2 nanoparticles in water can be made larger in size by polymer growth under simple experimental conditions to offer more sensitive detection by CE-UV, with the option of electrophoretic separation from organic compounds possibly found in water. In principle, our encapsulation technique (based on the polymerization of HPMA) may be affected by other components in the aqueous solution. However, it can be applied to real sample analysis. Samples would be prepared prior to polymerization to coat NPs. A filter of appropriate porosity can be used to remove soil particulates found in the water sample. The filtrate pH can be adjusted to the desired pH before starting the polymerization. The effect of salt will be removed in our future work by passing through a column of ion-exchange resin.

Transmission electron microscopy

Figure 8 shows the TEM images for SiO_2@PHPMA and SiO_2@PHPMA@PDA particles. A mean diameter of 14.6± 2.9 nm was found for SiO_2 nanoparticles. As shown in Fig. 8a, b, mean diameters of 18.6±2.2 and 20.1±1.6 nm were obtained for SiO_2@PHPMA and SiO_2@PHPMA@PDA, respectively. The thickness of PHPMA coating on the surface of SiO_2 nanoparticles was approximately 2±0.4 nm, whereas PDA coating on top of PHPMA was about 0.8±0.3 nm. The diameters of these dry particles, as determined by TEM, seem to be much smaller than the corresponding hydrodynamic diameters obtained by DLS measurement for particles in aqueous suspensions. Particles in liquid media develop a hydration layer around their surfaces, which impacts on their movement under the influence of Brownian motion. As this hydration layer is not present in TEM analysis, smaller diameters were obtained.

Conclusions

This work has demonstrated a new analytical approach to enhance the sensitivity for CE-UV detection of colloidal SiO_2 nanoparticles in water by coating with PHPMA alone or with the assistance of PDA, BPA, and PVA. The problem of inadequate sensitivity was broken down into smaller attempts toward technically simple and operationally cost-effective solutions. Experimental results have demonstrated the

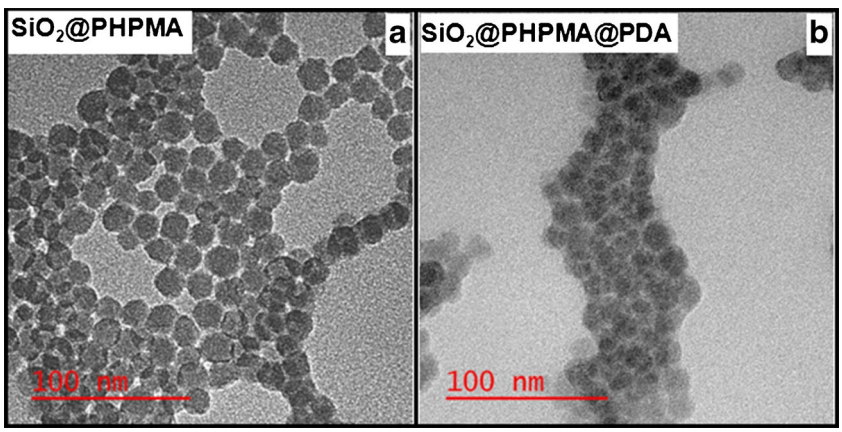

Fig. 8 Transmission electron micrographs of **a** SiO_2@PHPMA and **b** SiO_2@PHPMA@PDA

feasibility of an approach that can potentially be applied for the determination of other NMs and NPs in water analysis. Controlled growth of thicker polymer coatings is underway in our lab to attain complete coating, which would offer higher sensitivity needed for the detection of lower concentrations of NPs. Our ultimate objective is the implementation of this new approach in toxicology research regarding nanomaterials in water, to gain a better understanding of their long-term impact on environmental sustainability and public health.

Acknowledgments Financial support from NSERC Canada is gratefully acknowledged. S. Alsudir thanks the Saudi Ministry of Higher Education for her scholarship.

References

1. Weber D, Sharma R, Botnaraş S, Pham DV, Steiger J, De Cola L (2013) Base-etch removal of a ligand shell in thin films of ZnO nanoparticles for electronic applications. J Mater Chem C 1:7111–7116
2. Gong ZG (2013) Nanotechnology application in sports. Adv Mat Res 662:186–189
3. Abramova A, Gedanken A, Popov V, Ooi EH, Mason TJ, Joyce EM, Beddow J, Bayazitov V (2013) A sonochemical technology for coating of textiles with antibacterial nanoparticles and equipment for its implementation. Mater Lett 96:121–124
4. Nagelreiter C, Valenta C (2013) Size analysis of nanoparticles in commercial O/W sunscreens. Int J Pharm 456(2):517–519
5. Sinclai R, Li H, Madsen S, Dai H (2013) HREM analysis of graphite-encapsulated metallic nanoparticles for possible medical applications. Ultramicroscopy 134:167–174
6. Bosch J, Luchini A, Pichini S, Tamburro D, Fredolini C, Liotta L, Petricoin E, Pacifici R, Facchiano F, Segura J, Garaci E, Gutiérrez-Gallego R (2013) Analysis of urinary human growth hormone (hGH) using hydrogel nanoparticles and isoform differential immunoassays after short recombinant hGH treatment: preliminary results. J Pharmaceut Biomed 85:194–197
7. Li Y, Zhang X, Deng C (2013) Functionalized magnetic nanoparticles for sample preparation in proteomics and peptidomics analysis. Chem Soc Rev 42:8517–8539
8. Liu J, Tian M, Liang Z (2013) DNA analysis based on the electrocatalytic amplification of gold nanoparticles. Electrochim Acta 113: 186–193
9. Li J, Zhao Z, Feng J, Gao J, Chen Z (2013) Understanding the metabolic fate and assessing the biosafety of MnO nanoparticles by metabonomic analysis. Nanotechnology 24:455102
10. Suliman YAO, Ali D, Alarifi S, Harrath AH, Mansour L, Alwasel SH (2013) Evaluation of cytotoxic, oxidative stress, proinflammatory and genotoxic effect of silver nanoparticles in human lung epithelial cells. Environ Toxicol. doi:10.1002/tox.21880
11. Valdiglesias V, Costa C, Sharma V, Kili G, Psaro E, Teixeira P, Dhawan A, Laffon B (2013) Comparative study on effects of two different types of titanium dioxide nanoparticles on human neuronal cells. Food Chem Toxicol 57:352–361
12. Wehling J, Volkmann E, Grieb T, Rosenauer A, Maas M, Treccani L, Rezwan K (2013) A critical study: assessment of the effect of silica particles from 15 to 500 nm on bacterial viability. Environ Pollut 176: 292–299
13. Wang J, Lu AH, Li M, Zhang W, Chen YS, Tian DX, Li WC (2013) Thin porous alumina sheets as supports for stabilizing gold nanoparticles. ACS Nano 7:4902–4910
14. Achatz DE, Heiligtag FJ, Li X, Link M, Wolfbeis OS (2010) Colloidal silica nanoparticles for use in click chemistry-based conjugations and fluorescent affinity assays. Sensors Actuators B Chem 150:211–219
15. Graf C, Gao Q, Schütz I, Noufele CN, Ruan W, Posselt U, Korotianskiy E, Nordmeyer D, Rancan F, Hadam S, Vogt A, Lademann J, Haucke V, Rühl E (2012) Surface functionalization of silica nanoparticles supports colloidal stability in physiological media and facilitates internalization in cells. Langmuir 28: 7598–7613
16. Bonacchi S, Genovese D, Juris R, Montalti M, Prodi L, Rampazzo E, Zaccheroni N (2011) Luminescent silica nanoparticles: extending the frontiers of brightness. Angew Chem Int Ed 50:4056–4066
17. Egerton TA (2013) The influence of surface alumina and silica on the photocatalytic degradation of organic pollutants. Catalysts 3: 338–362
18. Barceló D, Farré M (2012) Analysis and Risk of Nanomaterials in Environmental and Food Samples, Series: Comprehensive Analytical Chemistry. Elsevier 59: 1-415
19. Delay M, Barceló D, Farré M (2013) Analysis and risk of nanomaterials in environmental and food samples. Anal Bioanal Chem 405:7557–7558
20. Bouwmeester H, Lynch I, Marvin HJP, Dawson KA, Berges M, Braguer D, Byrne HJ, Casey A, Chambers G, Clift MJD, Elia G, Fernandes TF, Fjellsb LB, Hatto P, Juillerat L, Klein C, Kreyling WG, Nickel C, Riediker M, Stone V (2011) Minimal analytical characterization of engineered nanomaterials needed for hazard assessment in biological matrices. Nanotoxicology 5:1–11
21. Markus AA, Parsons JR, Roex EWM, Kenter GCM, Laane RWPM (2013) Predicting the contribution of nanoparticles (Zn, Ti, Ag) to the annual metal load in the Dutch reaches of the Rhine and Meuse. Sci Total Environ 456–457:154–160
22. Timerbaev AR, Hartinger CG, Keppler BK (2006) Metallodrug research and analysis using capillary electrophoresis. Trends Anal Chem 25:868–875
23. Harris DC (2006) Quantitative Chemical Analysis, Seventhth edn. W. H. FreeMan and Company, New York
24. DeMaleki Z, Lai EPC, Dabek-Zlotorzynska E (2010) Capillary electrophoresis characterization of molecularly imprinted polymer particles in fast binding with 17b-estradiol. J Sep Sci 33:2796–2803
25. Chu HH, Fu DC (1998) Preparation of poly(hydroxyethy1 methacrylate) and poly(hydroxypropy1 methacrylate) lattices. Macromol Rapid Commun 19:107–110
26. Ali AMI, Pareek P, Sewell L, Schmid A, Fujii S, Armes SP, Shirley IM (2007) Synthesis of poly(2-hydroxypropyl methacrylate) latex particles via aqueous dispersion polymerization. Soft Matter 3: 1003–1013
27. 420875 ALDRICH, LUDOX® AM colloidal silica, 30 wt. % suspension in H_2O. http://www.sigmaaldrich.com/catalog/product/aldrich/420875?lang=en&region=CA
28. Costa ROR, Vasconcelos WL (2001) Organic/inorganic nanocomposite star polymers via atom transfer radical polymerization of methyl methacrylate using octafunctional silsesquioxane cores. Macromolecules 34:5398–5407
29. Christian P, Giles MR, Griffiths RMT, Irvine DJ, Major RC, Howdle SM (2000) Free radical polymerization of methyl methacrylate in supercritical carbon dioxide using a pseudo-graft stabilizer: effect of monomer, initiator, and stabilizer concentrations. Macromolecules 33:9222–9227